

Spectroscopic determination of the s -wave scattering lengths of ^{86}Sr and ^{88}Sr

P. G. Mickelson, Y. N. Martinez, A. D. Saenz, S. B. Nagel, Y. C. Chen, and T. C. Killian
Rice University, Department of Physics and Astronomy, Houston, Texas, 77251

P. Pellegrini, and R. Côté
Department of Physics, U-3046, University of Connecticut, Storrs, CT, 06269-3046

(Dated: November 2, 2018)

Abstract

We report the use of photoassociative spectroscopy to determine the ground state s -wave scattering lengths for the main bosonic isotopes of strontium, ^{86}Sr and ^{88}Sr . Photoassociative transitions are driven with a laser red-detuned by up to 1400 GHz from the $^1S_0 - ^1P_1$ atomic resonance at 461 nm. A minimum in the transition amplitude for ^{86}Sr at -494 ± 5 GHz allows us to determine the scattering lengths $610 a_0 < a_{86} < 2300 a_0$ for ^{86}Sr and a much smaller value of $-1 a_0 < a_{88} < 13 a_0$ for ^{88}Sr .

Photoassociative spectroscopy (PAS) of ultracold gases, in which a laser field resonantly excites colliding atoms to ro-vibrational states of excited molecular potentials, is a powerful probe of atomic cold collisions [1]. Transition frequencies have been used to obtain dispersion coefficients of molecular potentials, which yield the most accurate value of the atomic excited-state lifetime [2, 3, 4]. Transition amplitudes are related to the wave-function for colliding ground state atoms [5, 6], and can be used to determine the ground state s -wave scattering length [7, 8, 9, 10, 11, 12].

The s -wave scattering length is a crucial parameter for determining the efficiency of evaporative cooling and the stability of a Bose-Einstein condensate (BEC). It also sets the scale for collisional frequency shifts, which can limit the accuracy and stability of atomic frequency standards.

The cold collision properties of alkaline-earth atoms like strontium, calcium, and magnesium, and atoms with similar electronic structure such as ytterbium, are currently the focus of intense study. These atoms possess narrow optical resonances that have great potential for optical frequency standards [13, 14, 15, 16, 17]. Laser-cooling on narrow transitions is an efficient route to high phase-space density [18, 19], and a BEC was recently produced with ytterbium [20]. Fundamental interest in alkaline-earth atoms is also high because their simple molecular potentials allow accurate tests of cold collision theory [21, 22, 23].

PAS of calcium [11] and ytterbium [12] was recently used to determine s -wave scattering lengths of these atoms. This paper reports the use of PAS to determine the ground state s -wave scattering lengths for the main bosonic isotopes of strontium, ^{86}Sr and ^{88}Sr , which have relative abundances of 10% and 83% respectively. We find a huge scattering length for ^{86}Sr of $610 a_0 < a_{86} < 2300 a_0$. Appreciable uncertainty comes from the value of C_6 for the ground state potential. In contrast, for ^{88}Sr we find $-1 a_0 < a_{88} < 13 a_0$. From the data, we also make an improved measurement [4] of the $5s5p^1P_1$ atomic lifetime ($\tau = 5.25 \pm 0.01$ ns). PAS results for ^{88}Sr , yielding a similar value of τ and a different value of a_{88} , were recently posted [24].

For PAS of strontium, atoms are initially trapped in a magneto-optical trap (MOT) operating on the 461 nm $^1S_0 - ^1P_1$ transition, as described in [4, 25]. We are able to produce pure samples of each isotope from the same atomic beam due to the intrinsic isotope selectivity of a MOT. For ^{86}Sr and ^{88}Sr respectively, about 7×10^7 and 2.5×10^8 atoms are trapped and cooled to 2 mK.

After this stage, the 461 nm laser-cooling light is extinguished, the field gradient is reduced to 0.1 G/cm, and 689 nm light for the $^1S_0 - ^3P_1$ intercombination-line MOT [26] is switched on. This MOT consists of three retro-reflected beams, each with a diameter of 2 cm and intensity of $400 - 800 \mu\text{W}/\text{cm}^2$. Initially, the frequency of the laser-cooling light is detuned from atomic resonance by about -1.3 MHz, and spectrally broadened with a ± 1.0 MHz sine-wave modulation.

During a 50 ms transfer and equilibration period, the field gradient and spectral modulation are linearly ramped to 0.8 G/cm and ± 0.7 MHz. The detuning is ramped to about -0.9 MHz. This yields about 4×10^7 ^{86}Sr atoms at a temperature of $5 \pm 1 \mu\text{K}$ or 1.5×10^8 ^{88}Sr atoms at a temperature of about $8 \pm 2 \mu\text{K}$. The peak density for both isotopes is about $2 \times 10^{11} \text{cm}^{-3}$. The intercombination-line MOT parameters are then held constant during an adjustable hold time. In the absence of PAS, the lifetime of atoms in the trap is about 500 ms, limited by background gas collisions.

The size of the atom cloud, the number of atoms, and thus the peak density are primarily determined with absorption imaging using the $^1S_0 - ^1P_1$ transition. We image along the direction of gravity, and transverse $1/\sqrt{e}$ density radii are $\sigma = 250 \mu\text{m}$ for ^{86}Sr and $\sigma = 400 \mu\text{m}$ for ^{88}Sr . To obtain information on the cloud dimension along gravity [27], an additional camera monitors fluorescence perpendicular to this direction. The cloud is smaller by approximately a factor of two in this axis.

To excite photoassociative resonances, a PAS laser, tuned to the red of the atomic $^1S_0 - ^1P_1$ transition at 461 nm, is applied to the atoms during hold times of 200–800 ms. When the PAS laser is tuned to a molecular resonance, photoassociation provides a loss mechanism for the MOT, decreasing the number of atoms. The PAS laser has negligible effect on the atom cloud size or temperature. When the PAS light is tuned far from a molecular resonance, it has no effect on the rate of loss from the trap.

PAS light is generated from an extended cavity diode laser at 922 nm using second-harmonic generation in a linear enhancement cavity [28]. The laser linewidth is 80 MHz in the blue on a millisecond time scale, which contributes significantly to the observed PAS resonance linewidths. The laser frequency is measured with a wavemeter that is regularly calibrated with the cooling laser whose frequency is locked to the atomic $^1S_0 - ^1P_1$ transition. The resulting 1-sigma statistical uncertainty for frequency measurements of the PAS laser is 200 MHz. There is also a comparable systematic uncertainty due to the sensitivity of the

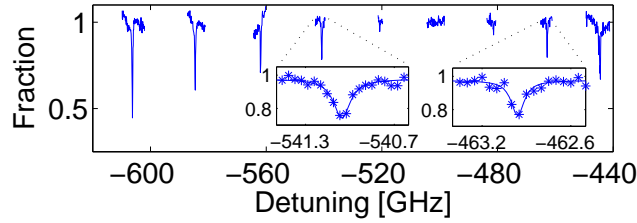


FIG. 1: Selected region of the ^{86}Sr PAS spectrum. The detuning is of the PAS laser with respect to the atomic $^1S_0 - ^1P_1$ transition frequency. The vertical axis is the fraction of atoms remaining at the end of the hold time in comparison to the number in the absence of photoassociation. PAS laser intensity is 800 mW/cm^2 , and hold times range from 350 to 450 ms. The minimum of the transition amplitude occurs when the Condon radius corresponds to a zero of the ground state wave function. The insets show the quality of the data and the fits to Eqs. 1 and 2.

wavemeter to the alignment of the laser into the device.

The available PAS laser power is as high as 20 mW. Several beam geometries are used, but typically the PAS beam is retroreflected, with a $1/e^2$ intensity radius of about $w = 1$ mm, yielding a maximum intensity of 3 W/cm^2 on the atoms. Lower intensities are obtained using an AOM. For some data, a quarter-wave plate is inserted in the beam path after the first pass through the atoms to prevent the formation of a standing wave. This variation has no noticeable affect on the PAS intensity and frequency measurements.

The observed PAS spectrum is relatively simple because the bosonic isotopes of strontium lack hyperfine structure. In addition, at the low temperatures of the intercombination-line MOT, only s -wave collisions occur so only $J = 1$ levels are excited. Ground state 1S_0 atoms collide on a $^1\Sigma_g^+$ potential, and, of the four states converging to the $^1S_0 + ^1P_1$ asymptote [21], only the $^1\Sigma_u^+$ state is excited in this work. Figure 1 shows spectra recorded for ^{86}Sr in a region around 500 GHz to the red of the atomic transition. The variation in transition amplitude will be discussed below, but first we describe the method used to quantitatively analyze the spectra.

The atom density varies as $\dot{n} = -\beta(I, f)n^2 - \Gamma n$, where f and I are the laser frequency and intensity. This implies the number of atoms in the trap as a function of hold time, t , follows

$$N(t) = \frac{N_0 e^{-\Gamma t}}{1 + \frac{n_0 \beta(I_{pk}, f) \zeta}{2\sqrt{2}\Gamma} (1 - e^{-\Gamma t})}, \quad (1)$$

where N_0 and n_0 are the number and peak density, respectively, at the beginning of the hold time. I_{pk} is the peak laser intensity, and $\zeta = w^2/(2\sigma^2 + w^2)$ accounts for the laser-atom overlap. We approximate the density distribution as a Gaussian. The one-body loss rate (Γ) and n_0 are fixed at values determined from independent measurements. Fit values of N_0 agree well with independent measurements and are a check of the method.

The photoassociative two-body loss rate, β , near resonance ν , is approximated as

$$\beta(I_{pk}, f) = \frac{2K_v I_{pk} \gamma_v}{\gamma} \frac{1}{1 + 4(f - f_v)^2/\gamma^2}, \quad (2)$$

where f_v is the center frequency for the transition. The experimental linewidth, $\gamma \approx 150$ MHz, approximately equals the sum of the natural radiative linewidth for the transition, $\gamma_v = 61$ MHz [4], and the measured laser linewidth. Including the factor γ_v/γ in Eq. 2 accounts for broadening beyond γ_v [29, 30]. I_{pk} is in units of mW/cm², and K_v is the collision rate constant, on resonance, for 1 mW/cm² intensity from an ideal laser with negligible linewidth. Difficulty in accurately determining the spatial dimensions of the atom cloud and in aligning the PAS laser beam on the atoms leads to systematic uncertainties of about a factor of two in measurements of K_v (Figs. 2 and 3). Except for the most intense PAS transitions close to atomic resonance for ⁸⁶Sr, the linear variation with intensity used in Eq. 2 is a good approximation and K_v is a constant for each transition.

From the observed transition frequencies we can obtain an accurate value of the atomic $5s5p^1P_1$ lifetime, τ . For the region of the molecular potentials probed by PAS, the transition energies can be described with the semiclassical approximation [31]

$$E(\nu) = D - X_0(\nu_D - \nu)^6, \\ X_0 = \left[\frac{\Gamma(4/3)}{2\sqrt{2\pi}\Gamma(5/6)} \right]^6 \frac{h^6}{\mu^3 C_3^2}, \quad (3)$$

where D is the dissociation energy, μ the reduced mass, $\lambda = 461$ nm, $C_3 = 3\hbar\lambda^3/16\pi^3\tau$, and ν_D is a non-integer quantum number corresponding to a hypothetical level at the dissociation limit. Relativistic retardation, rotational energy, higher order dispersion terms, ground state potential curvature, thermal shifts, and all light-induced shifts are negligible at our level of accuracy. A fit to the ⁸⁶Sr data yields $\tau = 5.25 \pm 0.01$ ns. The ⁸⁸Sr data is not extensive enough to contribute to the determination.

While all the data in Figs. 2 and 3 are valuable, the detunings of the laser corresponding to minima of the PAS rate are particularly important. At these detunings, the Condon radius

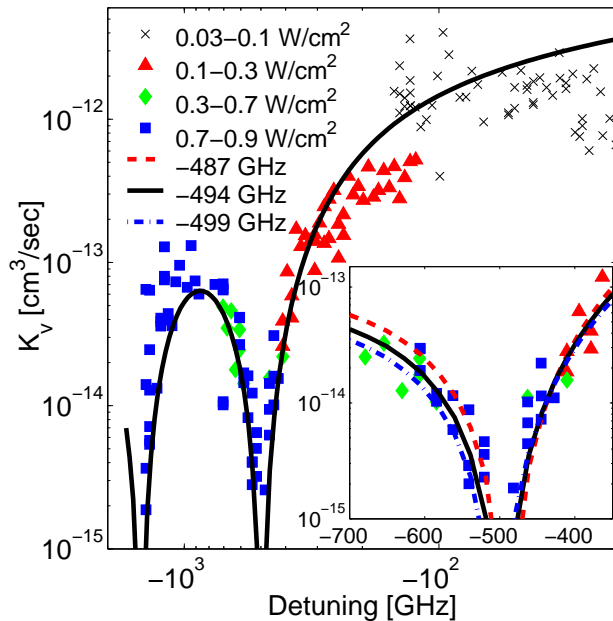


FIG. 2: Experimental and theoretical values for ^{86}Sr photoassociative rate constants for PAS laser intensities of 1 mW/cm^2 and a narrow laser linewidth. The experimental PAS laser intensity used for each measurement is indicated by the symbol. Theory is for $5\text{ }\mu\text{K}$ atoms with $C_6 = 3170\text{ a.u.}$ (Inset) Experimental amplitudes are scaled by $1/1.4$, which is reasonable given systematic uncertainties. The detuning of the minimum is used to determine the ground state potential as described in the text. The solid line is the best fit, corresponding to a minimum at -494 GHz . The dashed and dash-dot lines correspond to -487 GHz and -499 GHz respectively.

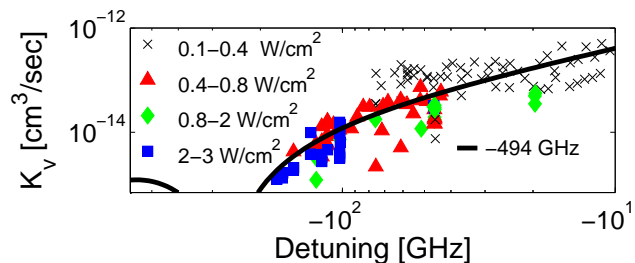


FIG. 3: Same as Fig. 2, but for ^{88}Sr . The theoretical curve, calculated for $10\text{ }\mu\text{K}$ atoms, is found using the potential determined from ^{86}Sr with $C_6 = 3170\text{ a.u.}$ It predicts a scattering length of $a_{88} = 6\text{ }a_0$.

for the excitation matches a node of the ground-state wave function, which is equivalent to saying the overlap integral between the ground- and excited-state wavefunctions vanishes. Minima positions provide precise enough information about ground-state potentials and wavefunctions to determine s -wave scattering lengths to high accuracy. The minima positions are also independent of atom density and laser intensity calibrations, and for the ultracold gases used here, they are independent of T , the temperature of the atoms.

For excitation by a laser with negligible linewidth, the collision rate constant at ultra-low temperatures and on resonance is [5]

$$K_v(T, I) = \frac{1}{hQ_T} \int_0^\infty d\epsilon e^{-\epsilon/k_B T} \frac{\gamma_v \gamma_s(\epsilon, J=0)}{(\epsilon^2 + (\gamma/2)^2)}, \quad (4)$$

where $Q_T = (2\pi\mu k_B T/h^2)^{3/2}$, k_B is the Boltzmann constant, $\gamma = \gamma_v + \gamma_s(\epsilon, J=0)$ with $\gamma_s(\epsilon, J=0)$ equal to the laser-stimulated width. At low laser intensities, $\gamma_s(\epsilon, J=0)$ can be expressed using Fermi's golden rule as $\gamma_s(\epsilon, J=0) = \pi I d^2 / \epsilon_0 c$. Here, ϵ_0 is the vacuum permittivity, c the vacuum speed of light and $d^2 = |\langle v | D(R) | \epsilon \rangle|^2$ where $D(R)$ is the molecular dipole transition moment connecting $|v\rangle$ and $|\epsilon\rangle$, the excited vibrational wave function and the energy normalized ground continuum wave function respectively. Because only bound levels close to the potential dissociation limit are excited, γ_v is independent of v and equal to twice the atomic linewidth γ_{at} . By the same argument, $D(R)$ can be approximated as independent of R [32] and is connected to the $^1S_0 - ^1P_1$ atomic dipole moment via $D(R) = \sqrt{2}\alpha d_{at}$. Using $d_{at} = \sqrt{3\pi\epsilon_0\hbar\gamma_{at}\lambda^3}$ and the line strength factor $\alpha = \sqrt{2/3}$ [21], we find $D = 3.6$ a.u.

For our analysis, the inner part ($R < 19 a_0$) of ground- and excited-state potentials are formed by an experimental RKR potential [33] and ab initio potential [34] respectively. These are smoothly connected to the multipolar van der Waals expansion in C_n/R^n at large internuclear separation. For the excited-state potential, only the C_3 term contributes, and we use the value determined above. For the ground-state potential, C_6 , C_8 and C_{10} terms are included [35, 36, 37]. Relativistic retardation effects in the asymptotic part of the excited-state potential are treated as described in [4]. Wave functions are calculated using a full quantum calculation. For the bound vibrational levels, the Mapped Fourier Grid Method [38] has been used whereas the ground-state continuum wave function was calculated using a Numerov algorithm.

Large transition moments for ^{86}Sr allow us to experimentally characterize about 80 tran-

sitions for this isotope, extending to detunings as large as -1400 GHz (Fig. 2). This allows us to clearly identify minima in the transition moment at -494 ± 5 GHz and -1500 GHz, corresponding to Condon radii of $62.6 \pm 0.2 a_0$ and $43 a_0$ respectively. To precisely determine the position of the minimum at -494 GHz, we calculated a set of potential curves with different node positions by varying the position of the repulsive inner-wall. Using these curves we performed a least-squares fit to the data shown in the inset of Fig. 2. Quoted uncertainties are one standard deviation. An overall amplitude factor was also varied but the best values were always well within the experimental uncertainties discussed above. The determined position of the node was independent of the value of the ground state C_6 coefficient used. It also did not change significantly if only data from -600 to -400 GHz was fit.

The Sr ground state potential determined from the node position and the ground state C_6 coefficient accurately describe the collisional properties of the system. This allows us to determine the s -wave scattering length a_{86} from the calculated zero-energy continuum wave function. However, we must carefully address the uncertainty in a_{86} arising from uncertainty in C_6 . The best values in the literature are a semiempirical method yielding $C_6 = 3250$ a.u. [36], and a relativistic many-body calculation of $C_6 = 3170$ a.u. [35], although a reevaluation of [35] inputting a more recent value of the $5s5p^1P_1$ lifetime [24] predicts $C_6 = 3103(7)$ a.u. [37]. If we take the latter value, and a minimum at -494 ± 5 GHz, we find $a_{86} = 1450_{-370}^{+850} a_0$. (a_{86} would diverge for a minimum position of -482 GHz.) This large scattering length indicates a bound level in the ground state potential very near threshold, which implies that a_{86} is also very sensitive to C_6 . For $C_6 = 3170$ a.u. and $C_6 = 3240$ a.u. we calculate $a_{86} = 940_{-170}^{+279} a_0$ and $a_{86} = 700_{-90}^{+140} a_0$ respectively. The spread in C_6 values makes it difficult to quote a rigorous statistical best value and uncertainty for a_{86} . Taking the extremes of the values found above, including spread in C_6 and one-standard-deviation variation in node position, we find $610 a_0 < a_{86} < 2300 a_0$.

PAS transitions in ^{88}Sr are significantly weaker than in ^{86}Sr , and only 50 transitions were characterized, extending to binding energies of -174 GHz (Fig. 3). We lack the sensitivity required to observe transitions to the red of the first minimum in the transition amplitude and thus cannot independently determine its position with high accuracy. However, the potential found using ^{86}Sr should also determine the wavefunctions for ^{88}Sr . Because of the heavy mass of strontium, effects due to the breakdown of the Born-Oppenheimer approximation should be negligible as is the case for rubidium [39]. Predicted photoassociation

rates agree with measurements within experimental uncertainties (Fig. 3), and we calculate $a_{88} = 10 \pm 3 a_0$ and a wave-function node at $76 \pm 0.4 a_0$ for $C_6 = 3103$ a.u. For $C_6 = 3240$ a.u., $a_{88} = 2 \pm 3 a_0$. This yields $-1 a_0 < a_{88} < 13 a_0$.

In conclusion, we determined the scattering lengths of ^{86}Sr and ^{88}Sr from PAS spectra. Our analysis uses full quantum calculations and is not based on semi-classical arguments [24, 40] that can be invalid if the scattering length becomes divergent (as in ^{86}Sr), small (as in ^{88}Sr), or negative. The large positive value for ^{86}Sr is very promising for the realization of a BEC through evaporative cooling in an optical trap. Such a condensate would have the advantage that losses due to inelastic processes would be minimal since there is no hyperfine interaction and spin-exchange collisions would not take place. The lifetime of a ^{86}Sr condensate would be influenced mostly by three-body recombination. BEC of ^{88}Sr will be a significant challenge [18] because of the small scattering length, but it may allow studies of a very weakly interacting quantum gas with behavior similar to a hydrogen condensate [41].

This research was supported by the Welch Foundation (Grant # C-1579), Office for Naval Research, and David and Lucille Packard Foundation. The authors are grateful to A. R. Allouche for providing them the Sr_2 ab initio potentials, and to E. Tiesinga and P. Julienne for valuable discussions.

-
- [1] J. Weiner *et al.*, Rev. Mod. Phys. **71**, 1 (1999).
 - [2] W. I. McAlexander *et al.*, Phys. Rev. A **51**, R871 (1995).
 - [3] K. M. Jones *et al.*, Europhys. Lett. **35**, 85 (1996).
 - [4] S. B. Nagel *et al.*, Phys. Rev. Lett. **94**, 083004 (2005).
 - [5] R. Napolitano *et al.*, Phys. Rev. Lett **73**, 1352 (1994).
 - [6] P. Julienne, J. Res. Natl. Inst. Stand. Technol. **101**, 487 (1996).
 - [7] J. R. Gardner *et al.*, Phys. Rev. Lett. **74**, 3764 (1995).
 - [8] E. R. I. Abraham *et al.*, Phys. Rev. A **55**, R3299 (1997).
 - [9] E. Tiesinga *et al.*, J. Res. Natl. Inst. Stand. Technol. **101**, 505 (1996).
 - [10] C. J. Williams *et al.*, Phys. Rev. A **60**, 4427 (1999).
 - [11] C. Degenhardt *et al.*, Phys. Rev. A **67**, 043408 (2003).

- [12] Y. Takasu *et al.*, Phys. Rev. Lett **93**, 123202 (2004).
- [13] H. Katori *et al.*, Phys. Rev. Lett. **91**, 173005 (2003).
- [14] M. Takamoto and H. Katori, Phys. Rev. Lett. **91**, 223001 (2003).
- [15] C. W. Oates *et al.*, Eur. Phys. J. D **7**, 449 (1999).
- [16] R. Santra *et al.*, physics/0411197 (2004).
- [17] T. Hong *et al.*, Phys. Rev. Lett. **94**, 50801 (2005).
- [18] T. Ido *et al.*, Phys. Rev. A **61**, 061403(R) (2000).
- [19] T. Mukaiyama *et al.*, Phys. Rev. Lett. **90**, 113002 (2003).
- [20] Y. Takasu *et al.*, Phys. Rev. Lett. **91**, 040404 (2003).
- [21] M. Machholm, P. S. Julienne, and K.-A. Suominen, Phys. Rev. A **64**, 033425 (2001).
- [22] R. Ciurylo *et al.*, Phys. Rev. A **70**, 062710 (2004).
- [23] R. W. Montalvão and R.J. Napolitano, Phys. Rev. A **64**, 011403(R) (2001).
- [24] M. Yasuda *et al.*, physics/0501053 (2005).
- [25] S. B. Nagel *et al.*, Phys. Rev. A **67**, 011401(R) (2003).
- [26] H. Katori *et al.*, Phys. Rev. Lett. **82**, 1116 (1999).
- [27] T. Loftus *et al.*, Phys. Rev. Lett. **93**, 073003 (2004).
- [28] M. Bode *et al.*, Opt. Lett. **22**, 1220 (1997).
- [29] C. McKenzie *et al.*, Phys. Rev. Lett. **88**, 120403 (2002).
- [30] U. Schloder *et al.*, Phys. Rev. A **66**, 061403(R) (2002).
- [31] R. J. Leroy and R. B. Bernstein, J. Chem. Phys. **52**, 3869 (1970).
- [32] E. Czuchaj, M. Krośnicki, and H. Stoll, Chem. Phys. Lett. **371**, 401 (2003).
- [33] G. Gerber, R. Möller, and H. Schneider, J. Chem. Phys. **81**, 1538 (1984).
- [34] N. Boutassetta, A. R. Allouche, and M. Aubert-Frécon, Phys. Rev. A **53**, 3845 (1996).
- [35] S. G. Porsev and A. Derevianko, Phys. Rev. A **65**, 020701(R) (2002).
- [36] J. Mitroy and M. W. J. Bromley, Phys. Rev. A **68**, 052714 (2003).
- [37] Private communication, A. Derevianko (2005).
- [38] V. Kokoouline *et al.*, J. Chem. Phys. **110**, 9865 (1999).
- [39] E. G. M. van Kempen *et al.*, Phys. Rev. Lett. **88**, 093201 (2002).
- [40] C. Boisseau *et al.*, Phys. Rev. A **62**, 052705 (2000).
- [41] D. G. Fried *et al.*, Phys. Rev. Lett. **81**, 3811 (1998).